Cluster Synthesis. 39. New Platinum–Ruthenium Carbonyl Cluster Complexes with Bridging Hydride Ligands. Synthesis and Structural Characterizations of $Ru_4Pt(CO)_{13}(COD)(\mu\text{-}H)_2$, $Ru_3Pt(CO)_9(\mu\text{-}CO)(COD)(\mu\text{-}H)_2$, $Ru_4Pt_2(CO)_{11}(COD)_2(\mu_3\text{-}H)_2$, and $Ru_5Pt_5(CO)_{18}(COD)_2(\mu\text{-}H)_2$, COD = Cycloocta-1,5-diene

Richard D. Adams,* Zhaoyang Li, Jau-Ching Lii, and Wengan Wu

Department of Chemistry and Biochemistry, University of South Carolina, Columbia, South Carolina 29208

Received February 6, 1992

The reaction of $Ru_4(CO)_{13}(\mu\text{-}H)_2$ (**1**) with $Pt(COD)_2$ at 25 °C yielded four new platinum–ruthenium carbonyl cluster complexes $Ru_4Pt(CO)_{13}(COD)(\mu\text{-}H)_2$ (**2**) (37%), $Ru_3Pt(CO)_9(\mu\text{-}CO)(COD)(\mu\text{-}H)_2$ (**3**) (10%), $Ru_4Pt_2(CO)_{11}(COD)_2(\mu_3\text{-}H)_2$ (**4**) (2.5%), and $Ru_5Pt_5(CO)_{18}(COD)_2(\mu_3\text{-}H)_2$ (**5**) (1%). All compounds were characterized by IR, ^1H NMR, and single-crystal X-ray diffraction analyses. The cluster of compound **2** consists of a butterfly tetrahedron of four ruthenium atoms with one triangular face capped by a Pt(COD) grouping. Compound **3** consists of a cluster of three ruthenium atoms and one platinum atom in a tetrahedral arrangement. Compound **4** consists of a tetrahedral cluster of four ruthenium atoms with two of the triangular faces capped by Pt(COD) groupings. The other two triangular faces have triply bridging hydride ligands. In the cluster of compound **5**, the five ruthenium and four of the platinum atoms are arranged in the form of a face-shared bioctahedron. The shared face consists of three of the platinum atoms. The fifth platinum atom is a cap on one of the Ru_2Pt triangles. Two hydride ligands are believed to bridge metals of the triangular faces on the opposite ends of the bioctahedron. Compounds **1**, **3**, and **4** were obtained in low yields by heating **2** to 68 °C. The yield of **3** was improved when **2** was heated to reflux in hexane solvent in the presence of $Pt(COD)_2$, but the yield of **4** was not changed significantly. Compound **4** was also obtained in a low yield (10%) from the reaction of $Ru_4(CO)_{12}(\mu\text{-}H)_4$ with $Pt(COD)_2$ in the presence of trimethylamine *N*-oxide. Crystal data: for **2** space group = $P\bar{1}$, a = 20.774 (3) Å, b = 15.364 (4) Å, c = 9.144 (1) Å, α = 95.60 (2)°, β = 102.68 (2)°, γ = 109.06 (3)°, Z = 2, 3076 reflections, R = 0.019; for **3** space group = $P\bar{1}$, a = 9.427 (2) Å, b = 14.102 (2) Å, c = 9.423 (2) Å, α = 95.24 (2)°, β = 116.70 (1)°, γ = 87.72 (2)°, Z = 2, 2180 reflections, R = 0.028; for **4** space group = $P2_1/c$, a = 9.261 (2) Å, b = 21.362 (7) Å, c = 16.307 (4) Å, β = 101.05 (2)°, 2887 reflections, R = 0.024; for **5**·C_6H_6 space group = $P2_1$, a = 12.338 (3) Å, b = 16.416 (4) Å, c = 12.792 (3) Å, β = 116.18 (2)°, 2801 reflections, R = 0.039.

Introduction

The chemistry of heteronuclear cluster complexes containing platinum has attracted a great deal of interest[1] because of the importance of bimetallic platinum alloys to the process of catalytic petroleum reforming.[2] Higher nuclearity mixed-metal clusters may serve as good models for such catalysts because the arrangement of the metal atoms on their surfaces may resemble those on the surfaces of real catalysts. It has recently been shown that $Pt(COD)_2$ can be a valuable reagent for the synthesis of heteronuclear cluster complexes containing platinum.[3-8] Our recent research has been focused on the study of high-nuclearity cluster complexes of platinum combined with a metal of the iron subgroup.[4-8] In this report our studies of the reactions of $Pt(COD)_2$ with the tetraruthenium cluster complex $Ru_4(CO)_{13}(\mu\text{-}H)_2$ (**1**) are described.

Experimental Section

General Procedures. All the reactions were performed under an atmosphere of nitrogen, unless otherwise indicated. Reagent grade solvents were dried over sodium and deoxygenated by purging with N_2 prior to use. $Pt(COD)_2$[9] was prepared by the reported procedure. $Ru_4(CO)_{13}(\mu\text{-}H)_2$ (**1**)[10] and $Ru_4(CO)_{12}(\mu\text{-}H)_4$[11] were prepared according to the literature. $Me_3NO{\cdot}2H_2O$ was purchased from Aldrich and was dehydrated by the published procedure before use.[12] IR spectra were recorded on a Nicolet 5DXB FT-IR spectrophotometer. ^1H NMR spectra were recorded on a Brüker AM-300 FT-NMR spectrometer. Elemental microanalyses were performed by Desert Analytics, Tucson, AZ. TLC separations were performed in air by using silica gel (60 Å, F_{254}) on plates (Whatman, 0.25 mm).

Reaction of 1 with $Pt(COD)_2$. A 50.0-mg sample of **1** (0.0649 mmol) was dissolved in 20 mL of hexane. Then 50.0 mg of $Pt(COD)_2$ (0.122 mmol) was added in several portions. The reaction was run at 25 °C for 1 h. The solvent was removed, and the residue was separated by TLC on silica gel with a hexane/CH_2Cl_2 (4/1) solvent mixture. This yielded in order of elution 26.0 mg of red-brown $Ru_4Pt(CO)_{13}(COD)(\mu\text{-}H)_2$ (**2**)

(1) (a) Farrugia, L. J. *Adv. Organomet. Chem.* **1990**, *31*, 301. (b) Braunstein, P.; Rose, J. In *Stereochemistry of Organometallic and Inorganic Compounds*; Bernal, I., Ed.; Elsevier: Amsterdam, 1989; Vol. 3.
(2) (a) Sinfelt, J. H. *Bimetallic Catalysts. Discoveries, Concepts and Applications*; Wiley: New York, 1983. (b) Sinfelt, J. H. *Sci. Am.* **1985**, *253*, 90. (c) Sinfelt, J. H. *Acc. Chem. Res.* **1977**, *10*, 15. (d) Sachtler, W. M. H. *J. Mol. Catal.* **1984**, *25*, 1. (e) Ponec, V. *Adv. Catal.* **1983**, *32*, 149. (f) Biswas, J.; Bickle, G. M.; Gray, P. G.; Do, D. D.; Barbier, J. *Catal. Rev.-Sci. Eng.* **1988**, *30*, 161.
(3) (a) Couture, C.; Farrar, D. H.; Goudsmit, R. J. *Inorg. Chim. Acta* **1984**, *89*, L29. (b) Couture, C.; Farrar, D. H. *J. Chem. Soc., Chem. Commun.* **1985**, 197. (c) Couture, C.; Farrar, D. H. *J. Chem. Soc., Dalton Trans.* **1986**, 1395. (d) Couture, C.; Farrar, D. H. *J. Chem. Soc., Dalton Trans.* **1987**, 2245. (e) Couture, C.; Farrar, D. H. *J. Chem. Soc., Dalton Trans.* **1987**, 2253.
(4) Adams, R. D.; Arafa, I.; Chen, G.; Lii, J. C.; Wang, J. G. *Organometallics* **1990**, *9*, 2350.
(5) Adams, R. D.; Chen, G.; Wang, J. G.; Wu, W. *Organometallics* **1990**, *9*, 1339.
(6) Adams, R. D.; Chen, G.; Lii, J. C.; Wu, W. *Inorg. Chem.* **1991**, *30*, 1007.
(7) Adams, R. D.; Lii, J. C.; Wu, W. *Inorg. Chem.* **1991**, *30*, 3613.
(8) Adams, R. D.; Alexander, M. S.; Arafa, I.; Wu, W. *Inorg. Chem.* **1991**, *30*, 4717.
(9) Spencer, J. L. *Inorg. Synth.* **1979**, *19*, 213.
(10) (a) Cauty, A. J.; Johnson, B. F. G.; Lewis, J. *J. Organomet. Chem.* **1972**, *43*, C35. (b) Cauty, A. J.; Johnson, B. F. G.; Lewis, J.; Norton, J. R. *J. Chem. Soc., Chem. Commun.* **1972**, 1331.
(11) Knox, S. A. R.; Koepke, J. W.; Andrews, M. A.; Kaesz, H. D. *J. Am. Chem. Soc.* **1975**, *97*, 3942.
(12) Smith, C.; Boekelheide. In *Organic Synthesis*; Wiley: New York, 1973; Collect. Vol. V, p 872.

0020-1669/92/1331-3445$03.00/0

Table I. Crystallographic Data for Diffraction Studies

compd	**2**	**3**	**4**	**5**
emp formula	$PtRu_4O_{13}C_{21}H_{14}$	$PtRu_3O_{10}C_{18}H_{14}$	$Pt_2Ru_4O_{11}C_{27}H_{26}$	$Pt_3Ru_5O_{18}C_{34}H_{26}\cdot C_6H_6$
fw	1073.70	888.60	1320.95	2281.48
cryst syst	triclinic	triclinic	monoclinic	monoclinic
lattice params				
a (Å)	20.774 (3)	9.427 (2)	9.261 (2)	12.338 (3)
b (Å)	15.364 (4)	14.102 (2)	21.362 (7)	16.416 (4)
c (Å)	9.144 (1)	9.423 (2)	16.307 (4)	12.792 (3)
α (deg)	95.60 (2)	95.24 (2)		90.00
β (deg)	102.68 (2)	116.70 (1)	101.05 (2)	116.18 (2)
γ (deg)	109.06 (3)	87.72 (2)		90.00
V (Å^3)	1372.2 (7)	1114.4 (8)	3166 (3)	2325 (2)
space group	$P\bar{1}$ (No. 2)	$P\bar{1}$ (No. 2)	$P2_1/c$ (No. 14)	$P2_1$ (No. 4)
Z	2	2	4	2
D_{calc} (g/cm^3)	2.60	2.65	2.77	3.26
μ(Mo Kα) (cm^{-1})	73.1	83.3	107.8	167.5
abs corr	empirical	empirical	empirical	empirical
temp (°C)	20	20	20	20
no. of observns				
($I > 3\sigma(I)$)	3076	2180	2887	2801
no. of variables	358	297	405	388
residuals:[a] R, R_w	0.019; 0.023	0.028; 0.037	0.024; 0.024	0.039; 0.041

[a] $R = \sum_{hkl}(||F_o| - |F_c||)/\sum|F_o|$; $R_w = (\sum_{hkl} w(|F_o| - |F_c|)^2/\sum_{hkl} w|F_o|^2)^{1/2}$.

(37%), 5.8 mg of yellow $Ru_3Pt(CO)_{10}(COD)(\mu\text{-}H)_2$ (**3**) (10%), 2.0 mg of brown-red $Ru_4Pt_2(CO)_{11}(COD)_2(\mu_3\text{-}H)_2$ (**4**) (2.5%), and 1.2 mg of gray-brown $Ru_5Pt_5(CO)_{18}(COD)_2(\mu_3\text{-}H)_2$ (**5**) (1%). IR (ν_{CO}): for **2** (in hexane) 2095 (m), 2072 (vs), 2032 (vs), 2029 (vs), 2018 (w), 2008 (m), 1982 (w), 1945 (vw), 1932 (w); for **3** (in hexane) 2088 (m), 2060 (vs), 2040 (vs), 2023 (m), 2017 (w), 2004 (s), 1990 (vw), 1910 (vw), 1829 (m); for **4** (in hexane) 2040 (w), 2032 (w), 2016 (vs), 2003 (m), 1978 (w), 1964 (w), 1947 (vw), 1866 (w); for **5** (in CH_2Cl_2) 2072 (s), 2040 (s), 2023 (vs), 1992 (w). ^{1}H NMR (δ): for **2** (in $CDCl_3$) 5.6–5.9 (m, 4 H, $^2J_{Pt-H}$ = 36 Hz), 2.0–3.0 (m, 8 H), −16.93 (t, 2 H, $^2J_{Pt-H}$ = 29 Hz); for **3** (in $CDCl_3$) 5.2–5.4 (m, 4 H, $^2J_{Pt-H}$ = 44 Hz), 2.4–3.0 (m, 8 H), −20.78 (t, 2 H, $^2J_{Pt-H}$ = 29 Hz); for **4** (in $CDCl_3$) 5.5–5.7 (m, 8 H, $^2J_{Pt-H}$ = 59 Hz), 2.1–2.6 (m, 16 H), −19.3 (t, 2 H, $^2J_{Pt-H}$ = 17 Hz); for **5** (in CD_2Cl_2 at −80 °C) 5.6–5.9 (m, 8 H, $^2J_{Pt-H}$ = 44 Hz), 2.3–2.7 (m, 16 H), −18.46 (s, 1 H), −23.82 (s, 1 H). Anal. Calc (found) for **2**: C, 23.49 (23.73); H, 1.31 (1.30). Calc (found) for **3**: C, 24.33 (24.23); H, 1.59 (1.82). Calc (found) for **4**: C, 24.55 (24.58); H, 1.98 (1.82). Calc (found) for **5**: C, 18.55 (18.89); H, 1.10 (1.02).

Pyrolysis of 2 at 68 °C. A 21.5-mg (0.020-mmol) sample of **2** was dissolved in 30 mL of hexane, and then the solution was heated to reflux for 35 min. The solvent was removed in vacuo, and the residue was chromatographed by TLC (hexane/CH_2Cl_2 = 4/1). This yielded in order of elution 1.2 mg of a mixture of $Ru_4(CO)_{12}(\mu\text{-}H)_4$ and $Ru_3(CO)_{12}$, 1.7 mg of orange-red **1** (11%), a trace of starting material **2**, 0.3 mg of an uncharacterizable brown-gray compound [IR (ν_{CO} in hexane): 2067 (vs), 2047 (w), 2033 (w)], 1.2 mg of **3** (7%), 0.5 mg of a brown unknown mixture, 0.4 mg of orange $Ru_4Pt(CO)_{13}(COD)$ (**6**)[8] (2%), and 0.9 mg of **4** (7%).

Reaction of 2 with Pt(COD)$_2$. A 21.0-mg sample of **2** (0.020 mmol) was dissolved in 45 mL of CH_2Cl_2. Then 21.0 mg of $Pt(COD)_2$ (0.051 mmol) was added to the solution, and the reaction mixture was heated to reflux under nitrogen for 1.0 h. At this time a second portion of 21.0 mg of $Pt(COD)_2$ was added and the solution was allowed to stir for another 2.0 h. The mixture was separated by TLC with a hexane/CH_2Cl_2 (3/1) solvent mixture to yield in order of elution 1.8 mg of unreacted **2** (9%), 3.0 mg of **3** (17%), and 1.5 mg of **4** (6%).

Reaction of Ru$_4$(CO)$_{12}$(μ-H)$_4$ with Pt(COD)$_2$ and Me$_3$NO. A 15.0-mg sample of $Ru_4(CO)_{12}(\mu\text{-}H)_4$ (0.02 mmol) was dissolved in 20 mL of CH_2Cl_2, and 1.5 mg of Me_3NO (0.0200 mmol) was added. The solution turned to orange-red. After 30 min, 40.0 mg of $Pt(COD)_2$ (0.0973 mmol) was added. The solution was allowed to stir at 25 °C for 10 min. Solvent was removed, and the residue was chromatographed by TLC (hexane/CH_2Cl_2 = 4/1) to yield 3.4 mg of unreacted $Ru_4(CO)_{12}(\mu\text{-}H)_4$ and 2.6 mg of **4** (10%).

Crystallographic Analyses. Crystals of compounds **2**–**4** suitable for diffraction analyses were grown by slow evaporation of solvent from a solution of CH_2Cl_2/hexane (5/1) at 25 °C. Crystals of compound **5** were grown in a solution of CH_2Cl_2/benzene (4/1) mixture solvent at 10 °C. All data crystals were mounted in thin-walled glass capillaries. Diffraction measurements were made on a Rigaku AFC6S fully automated four-circle diffractometer using graphite-monochromated Mo Kα radiation. Unit cells were determined and refined from 15 randomly selected reflections obtained by using the AFC6S automatic search, center, index, and least-squares routines. Intensity data were collected by using the ω-scan technique (moving crystal–stationary counter). All data processing was performed on a Digital Equipment Corp. VAXstation 3520 computer by using the TEXSAN structure-solving program library (version 5.0) obtained from Molecular Structure Corp., Woodlands, TX. Neutral-atom scattering factors were calculated by the standard procedures.[13a] Anomalous dispersion corrections were applied to all non-hydrogen atoms.[13b] Lorentz/polarization (*Lp*) and absorption corrections (empirical based on azimuthal scans of three reflections) were applied to the data for each structure. Full-matrix least-squares refinements minimized the function $\sum_{hkl} w(|F_o| - |F_c|)^2$, where $w = 1/\sigma(F_o)^2$, $\sigma(F_o) = \sigma(F_o^2)/2F_o$, and $\sigma(F_o^2) = [\sigma(I_{raw})^2 + (0.02I_{net})^2]^{1/2}/Lp$. For each structure the hydrogen atoms on the COD ligands were calculated by using idealized geometries. The contributions of these atoms were added to the structure factor calculations, but their positions were not refined.

Compounds **2** and **3** crystallized in the triclinic crystal system. The space group $P\bar{1}$ was assumed and confirmed by the successful solution and refinement of the structures. Both of the structures were solved by a combination of direct methods (MITHRIL) and difference Fourier syntheses. All non-hydrogen atoms in both of these two structures were refined with anisotropic thermal parameters. For both structures the hydride ligands were located in a difference Fourier synthesis. For **2** the hydride ligands were refined on their positional parameters only. For **3** the hydride ligands were refined both on their positional parameters and by using an isotropic thermal parameter.

Compounds **4** and **5** crystallized in the monoclinic crystal system. Both structures were solved by a combination of direct methods (MITHRIL) and difference Fourier syntheses. For **4**, the space group $P2_1/c$ was established on the basis of the systematic absences observed during the collection of the data. All non-hydrogen atoms were refined with anisotropic thermal parameters. The hydride ligands were located in a difference Fourier synthesis and were refined successfully with isotropic thermal parameters.

For **5**, the systematic absences in the data were consistent with either of the space groups $P2_1/m$ or $P2_1$. Efforts to solve the structure in the space group $P2_1/m$ were unsuccessful. The space group $P2_1$ was thus assumed and subsequently confirmed by the successful solution and refinement of the structure. All atoms heavier than carbon were refined with anisotropic thermal parameters. In the final stages of the analysis a molecule of benzene that cocrystallized from the crystallization solvent was located in the lattice. It was refined partially, but this model would not converge and the benzene therefore was included as a fixed contribution in the final analysis. The hydride ligands were not located in this analysis and were ignored.

(13) *International Tables for X-ray Crystallography*; Kynoch Press: Birmingham, England, 1975; Vol. IV, (a) Table 2.2B, pp 99–101, (b) Table 2.3.1, pp 149–150.

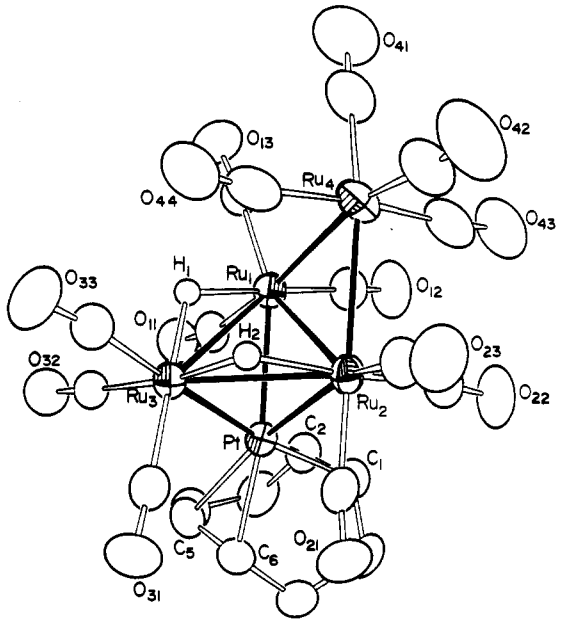

Figure 1. ORTEP drawing of $Ru_4Pt(CO)_{13}(COD)(\mu\text{-}H)_2$ (**2**) showing 50% probability thermal ellipsoids.

Table II. Positional Parameters and B(eq) Values for **2**

atom	x	y	z	B(eq)[a] (Å^2)
Pt	0.36339 (2)	0.192575 (15)	0.79235 (2)	2.693 (9)
Ru(1)	0.53885 (5)	0.18185 (3)	0.62193 (5)	2.82 (2)
Ru(2)	0.61826 (5)	0.34529 (3)	0.84891 (5)	2.82 (2)
Ru(3)	0.38105 (5)	0.30603 (3)	0.58641 (5)	2.52 (2)
Ru(4)	0.80078 (5)	0.32661 (4)	0.67055 (7)	4.07 (2)
H(1)	0.464 (5)	0.249 (3)	0.502 (5)	3.0
H(2)	0.538 (5)	0.383 (3)	0.682 (5)	3.0

[a] $B_{eq} = 8\pi^2/3\sum_{i=1}^{3}\sum_{i=1}^{3} U_{ij}a_i^*a_j^*\vec{a}_i\vec{a}_j$. See: Fischer R. X.; Tillmanns, E. *Acta Crystallogr.* **1988**, *C44*, 775.

Table III. Intramolecular Distances (Å) for **2**[a]

Pt–Ru(1)	2.7341 (8)	Ru(2)–Ru(4)	2.8800 (9)
Pt–Ru(2)	2.872 (1)	Ru(2)–C(21)	1.905 (7)
Pt–Ru(3)	2.6837 (8)	Ru(2)–C(22)	1.907 (7)
Pt–C(1)	2.272 (6)	Ru(2)–C(23)	1.900 (7)
Pt–C(2)	2.303 (6)	Ru(2)–H(2)	1.83 (5)
Pt–C(5)	2.204 (6)	Ru(3)–C(31)	1.904 (6)
Pt–C(6)	2.199 (6)	Ru(3)–C(32)	1.893 (7)
Pt–C(11)	2.541 (6)	Ru(3)–C(33)	1.928 (7)
Pt–C(21)	2.764 (6)	Ru(3)–H(1)	1.69 (4)
Ru(1)–Ru(2)	2.854 (1)	Ru(3)–H(2)	1.69 (5)
Ru(1)–Ru(3)	2.938 (1)	Ru(4)–C(41)	1.918 (8)
Ru(1)–Ru(4)	2.875 (1)	Ru(4)–C(42)	1.900 (8)
Ru(1)–C(11)	1.900 (7)	Ru(4)–C(43)	1.952 (9)
Ru(1)–C(12)	1.880 (7)	Ru(4)–C(44)	1.931 (8)
Ru(1)–C(13)	1.902 (7)	C(1)–C(2)	1.386 (8)
Ru(1)–H(1)	1.81 (5)	C(5)–C(6)	1.381 (8)
Ru(2)–Ru(3)	2.946 (1)	O–C(av)	1.137 (9)

[a] Estimated standard deviations in the least significant figure are given in parentheses.

Results

From the reaction of $Ru_4(CO)_{13}(\mu\text{-}H)_2$ (**1**) with $Pt(COD)_2$ at 25 °C we have obtained four new platinum–ruthenium carbonyl cluster complexes: $Ru_4Pt(CO)_{13}(COD)(\mu\text{-}H)_2$ (**2**) (37%), $Ru_3Pt(CO)_9(\mu\text{-}CO)(COD)(\mu\text{-}H)_2$ (**3**) (10%), $Ru_4Pt_2(CO)_{11}(COD)_2(\mu_3\text{-}H)_2$ (**4**) (2.5%), and $Ru_5Pt_5(CO)_{18}(COD)_2(\mu_3\text{-}H)_2$ (**5**) (1%). All four compounds were characterized by IR, ^{1}H NMR, and single-crystal X-ray diffraction analyses. The major product is **2**, and an ORTEP diagram of its molecular structure is shown in Figure 1. Final atom positional parameters are listed in Table II. Selected interatomic distances and angles are listed in Tables III and IV. The cluster of compound **2** consists of a butterfly tetrahedron of four ruthenium atoms with one of the triangular faces capped by a Pt(COD) grouping. It could alternatively be viewed as a Ru_3Pt tetrahedron with an edge-bridging $Ru(CO)_4$ grouping. The cluster is structurally very similar to the compound $Ru_4Pt(CO)_{12}(\mu_4\text{-}CO)(COD)$ (**6**) that was recently reported by us,[8] except that **6** contains a quadruply bridging carbonyl ligand in the fold of the butterfly and **2** has two bridging hydride ligands. The hydride ligands in **2** were located and refined structurally, $\delta = -16.93$, $^2J_{Pt\text{-}H} = 29$ Hz. They bridge the Ru(1)–Ru(3) and R(2)–Ru(3) bonds and produce the usual lengthening effect on these bonds.[14] They exhibit the same chemical shift in solution due to the approximate reflection plane (not a crystallographic plane) that passes through the molecule and includes the metal atoms Ru(4) and Pt. The Pt–Ru bond distances in **2** span a wider range, 2.6837 (8)–2.872 (1) Å than those in **6**, 2.714 (1)–2.819 (1) Å. The Ru–Ru distances to Ru(4) are significantly longer, 2.875 (1) and 2.880 (1) Å, than corresponding distances in **6**, 2.816 (1) and 2.818 (1) Å. The shorter lengths in **6** can be attributed to the presence of the CO ligand that bridges to this metal atom. The molecule contains a total of 74 valence electrons which is exactly the value expected for a capped butterfly tetrahedron of five metal atoms.[15]

Table IV. Intramolecular Bond Angles (deg) for **2**[a]

Ru(1)–Pt–Ru(2)	61.15 (2)	Pt–Ru(2)–Ru(4)	117.21 (3)
Ru(1)–Pt–Ru(3)	65.68 (2)	Ru(1)–Ru(2)–Ru(3)	60.85 (3)
Ru(2)–Pt–Ru(3)	63.94 (2)	Ru(1)–Ru(2)–Ru(4)	60.18 (3)
Pt–Ru(1)–Ru(2)	61.80 (3)	Ru(3)–Ru(2)–Ru(4)	95.63 (3)
Pt–Ru(1)–Ru(3)	56.33 (2)	Pt–Ru(3)–Ru(1)	57.99 (2)
Pt–Ru(1)–Ru(4)	122.13 (3)	Pt–Ru(3)–Ru(2)	61.13 (3)
Ru(2)–Ru(1)–Ru(3)	61.11 (2)	Ru(1)–Ru(3)–Ru(2)	58.03 (3)
Ru(2)–Ru(1)–Ru(4)	60.36 (3)	Ru(1)–Ru(4)–Ru(2)	59.46 (3)
Ru(3)–Ru(1)–Ru(4)	95.90 (3)	Ru(1)–C(11)–O(11)	165.5 (5)
Pt–Ru(2)–Ru(1)	57.05 (3)	Ru(2)–C(21)–O(21)	168.4 (5)
Pt–Ru(2)–Ru(3)	54.93 (3)	Ru–C(av)–O	175.4 (8)

[a] Estimated standard deviations in the least significant figure are given in parentheses.

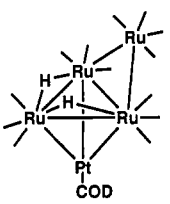

2

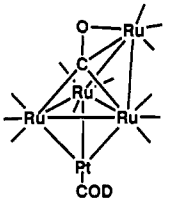

6

When heated, compound **2** eliminates an $Ru(CO)_3$ grouping to yield compound **3** (7%) and competitively eliminates a Pt(COD) grouping to reform **1** (11%). The structure of **3** is analogous to the homologous osmium compound $Os_3Pt(CO)_9(\mu\text{-}CO)(COD)(\mu\text{-}H)_2$ (**7**).[16] An ORTEP diagram of the structure of **3** is shown in Figure 2. Final atom positional parameters are listed in Table V. Selected interatomic distances and angles are listed in Tables VI and VII. The structure consists of a tetrahedral Ru_3Pt cluster with hydride ligands bridging two of the ruthenium–ruthenium bonds and a CO ligand bridging the remaining Ru–Ru bond in the site formerly occupied by the $Ru(CO)_4$ grouping in **2**. The hydride-bridged Ru–Ru bonds are long as expected, and there is considerably less scatter in the Pt–Ru distance than that found in **2**, Pt–Ru range = 2.718 (1)–2.7942 (9) Å. The CO-bridged Ru–Ru bond, 2.810 (1) Å, is significantly shorter than the corresponding distance in **2**, 2.854 (1) Å. C(22)–O(22) is a strong semibridging ligand to Pt, Pt···C(22) = 2.35 (1) Å, while C(13) is a slightly weaker semibridge to Pt, Pt···C(13) =

(14) Churchill, M. R. In *Transition Metal Hydrides*; Advances in Chemistry Series No. 167; American Chemical Society: Washington, DC, 1978.
(15) Mingos, D. M. P.; May, A. S. In *The Chemistry of Metal Cluster Complexes*; Shriver, D. F., Kaesz, H. D., Adams, R. D., Eds.; VCH Publishers: New York, 1990; Chapter 2.
(16) Ewing, P.; Farrugia, L. J. *J. Organomet. Chem.* **1988**, *347*, C31.

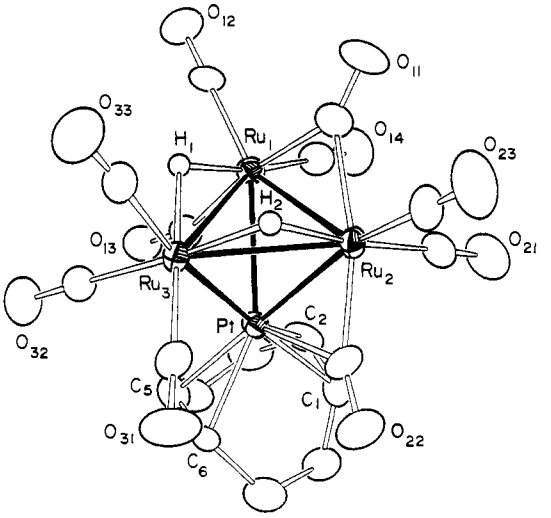

Figure 2. ORTEP diagram of $Ru_3Pt(CO)_{10}(COD)(\mu\text{-}H)_2$ (**3**) showing 50% probability thermal ellipsoids.

Table V. Positional Parameters and *B*(eq) Values for **3**

atom	*x*	*y*	*z*	*B*(eq)[a] (Å²)
Pt	0.80589 (3)	0.22126 (2)	0.22057 (4)	1.77 (2)
Ru(1)	0.76882 (8)	0.38143 (5)	0.05306 (8)	1.91 (3)
Ru(2)	0.92079 (8)	0.21598 (5)	0.00088 (8)	1.92 (3)
Ru(3)	1.07424 (8)	0.32469 (5)	0.31022 (8)	1.75 (3)
H(1)	0.956 (9)	0.421 (6)	0.197 (9)	3 (1)
H(2)	1.100 (9)	0.281 (6)	0.143 (10)	3 (1)

[a] $B_{eq} = 8\pi^2/3\sum_{i=1}^{3}\sum_{j=1}^{3}U_{ij}a_i^*a_j^*\vec{a}_i\vec{a}_j$. See: Fishcer, R. X.; Tillmanns, E. *Acta Crystallogr.* **1988**, *C44*, 775.

Table VI. Intramolecular Distances (Å) for **3**[a]

Pt–Ru(1)	2.7942 (9)	Ru(1)–H(1)	1.75 (8)
Pt–Ru(2)	2.7284 (9)	Ru(2)–Ru(3)	2.918 (1)
Pt–Ru(3)	2.718 (1)	Ru(2)–C(11)	2.14 (1)
Pt–C(1)	2.32 (1)	Ru(2)–C(21)	1.87 (1)
Pt–C(2)	2.303 (8)	Ru(2)–C(22)	1.98 (1)
Pt–C(5)	2.227 (9)	Ru(2)–C(23)	1.92 (1)
Pt–C(6)	2.222 (8)	Ru(2)–H(2)	1.83 (8)
Pt–C(13)	2.50 (1)	Ru(3)–C(31)	1.90 (1)
Pt–C(22)	2.35 (1)	Ru(3)–C(32)	1.90 (1)
Ru(1)–Ru(2)	2.810 (1)	Ru(3)–C(33)	1.92 (1)
Ru(1)–Ru(3)	2.950 (1)	Ru(3)–H(1)	1.81 (8)
Ru(1)–C(11)	2.10 (1)	Ru(3)–H(2)	1.75 (8)
Ru(1)–C(12)	1.91 (1)	C(1)–C(2)	1.39 (1)
Ru(1)–C(13)	1.97 (1)	C(5)–C(6)	1.36 (1)
Ru(1)–C(14)	1.89 (1)	O–C(av)	1.14 (1)

[a] Estimated standard deviations in the least significant figure are given in parentheses.

Table VII. Intramolecular Bond Angles (deg) for **3**[a]

Ru(1)–Pt–Ru(2)	61.15 (2)	Pt–Ru(3)–Ru(1)	58.90 (2)
Ru(1)–Pt–Ru(3)	64.70 (3)	Pt–Ru(3)–Ru(2)	57.78 (2)
Ru(2)–Pt–Ru(3)	64.78 (3)	Ru(1)–Ru(3)–Ru(2)	57.22 (3)
Pt–Ru(1)–Ru(2)	58.27 (2)	Ru(1)–C(11)–O(11)	140.3 (8)
Pt–Ru(1)–Ru(3)	56.40 (3)	Ru(2)–C(11)–O(11)	136.6 (8)
Ru(2)–Ru(1)–Ru(3)	60.80 (3)	Ru(1)–C(13)–O(13)	157.5 (8)
Pt–Ru(2)–Ru(1)	60.58 (2)	Pt–C(22)–O(22)	128.6 (8)
Pt–Ru(2)–Ru(3)	57.44 (2)	Ru(2)–C(22)–O(22)	153.9 (8)
Ru(1)–Ru(2)–Ru(3)	61.98 (3)	Ru–C(av)–O	177.6 (9)

[a] Estimated standard deviations in the least significant figure are given in parentheses.

2.50 (1) Å. Compound **4** which has two platinum atoms was also formed (7%) when **2** was heated to 68 °C. Its formation helps to account for the fate of some of the Pt(COD) that was lost from **2** in the regeneration of **1**.

An ORTEP diagram of the structure of **4** is shown in Figure 3. Final atom positional parameters are listed in Table VIII. Selected interatomic distances and angles are listed in Tables IX and X. The cluster consists of a tetrahedral group of four ruthenium

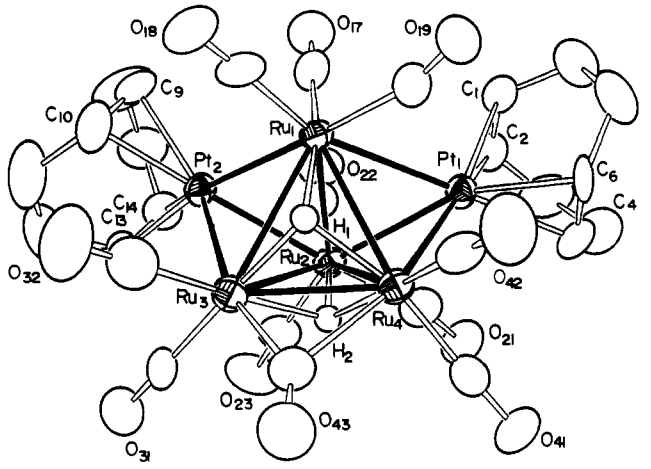

Figure 3. ORTEP diagram of $Ru_4Pt_2(CO)_{11}(COD)_2(\mu_3\text{-}H)_2$ (**4**) showing 50% probability thermal ellipsoids.

Table VIII. Positional Parameters and *B*(eq) Values for **4**

atom	*x*	*y*	*z*	*B*(eq)[a] (Å²)
Pt(1)	0.33167 (4)	0.156179 (20)	0.58264 (2)	2.44 (2)
Pt(2)	0.21983 (4)	0.016116 (20)	0.78598 (2)	2.51 (2)
Ru(1)	0.13508 (8)	0.07207 (4)	0.63505 (5)	2.25 (3)
Ru(2)	0.37856 (8)	0.11619 (4)	0.75140 (5)	2.36 (4)
Ru(3)	0.08065 (9)	0.13497 (4)	0.79440 (5)	2.69 (4)
Ru(4)	0.14971 (9)	0.20776 (4)	0.67235 (5)	2.48 (4)
H(1)	0.050 (8)	0.136 (4)	0.683 (4)	2 (1)
H(2)	0.249 (9)	0.175 (4)	0.765 (5)	3.2 (9)

[a] $B_{eq} = 8\pi^2/3\sum_{i=1}^{2}\sum_{j=1}^{3}U_{ij}a_i^*a_j^*\vec{a}_i\vec{a}_j$. See: Fischer, R. X.; Tillmanns, E. *Acta Crystallogr.* **1988**, *C44*, 775.

atoms with Pt(COD) groupings capping two of the triangular Ru_3 faces. In addition there are two triply bridging hydride ligands (located and refined structurally, $\delta = -19.3$, $^2J_{Pt-H} = 17$ Hz) that span the two remaining Ru_3 faces of the Ru_4 tetrahedron. The structure is very similar to the compound $Ru_6(CO)_{17}(\mu_3\text{-}H)_2$ (**8**)

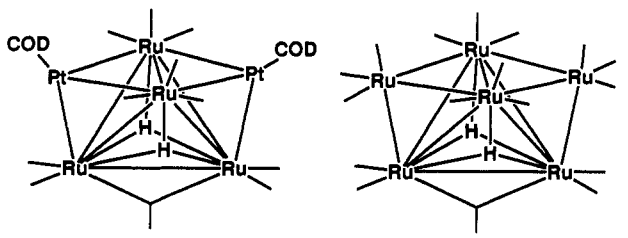

4 **8**

that was recently reported by McCarthy et al.[17] There is a bridging carbonyl ligand across the Ru(3)–Ru(4) bond which is also quite short, Ru(3)–Ru(4) = 2.698 (1) Å, but the corresponding distance observed in **8** was even shorter, 2.643 (1) Å. The compound contains 84 valence electrons which is the number expected for a bicapped tetrahedron.[15]

One very minor product, compound **5**, was also isolated from the original reaction of **1** with $Pt(COD)_2$. This is a high-nuclearity species containing ten metal atoms, five rutheniums, and five platinums. We were unable to devise a better yield synthesis of **5**; studies of this compound therefore were limited due to the small amounts that could obtained. An ORTEP diagram of the structure of **5** is shown in Figure 4. Final atom positional parameters are listed in Table XI. Selected interatomic distances and angles are listed in Tables XII and XIII. The cluster of compound **5** can be described as a face-shared bioctahedron with one capping group. The shared face contains three of the five

(17) McCarthy, D. A.; Krause, J. K.; Shore, S. G. *J. Am. Chem. Soc.* **1990**, *112*, 8587.

Table IX. Intramolecular Distances (Å) for **4**[a]

Pt(1)–Ru(1)	2.805 (1)	Ru(2)–Ru(3)	3.001 (1)
Pt(1)–Ru(2)	2.834 (1)	Ru(2)–Ru(4)	2.989 (1)
Pt(1)–Ru(4)	2.672 (1)	Ru(2)–C(21)	1.96 (1)
Pt(1)–C(1)	2.27 (1)	Ru(2)–C(22)	1.89 (1)
Pt(1)–C(2)	2.28 (1)	Ru(2)–C(23)	1.88 (1)
Pt(1)–C(5)	2.17 (1)	Ru(2)–H(2)	1.78 (8)
Pt(1)–C(6)	2.176 (9)	Ru(3)–Ru(4)	2.698 (1)
Pt(1)–C(19)	2.53 (1)	Ru(3)–C(31)	1.87 (1)
Pt(1)–C(21)	2.64 (1)	Ru(3)–C(32)	1.85 (1)
Pt(2)–Ru(1)	2.713 (1)	Ru(3)–C(43)	2.01 (1)
Pt(2)–Ru(2)	2.714 (1)	Ru(3)–H(1)	1.79 (7)
Pt(2)–Ru(3)	2.863 (1)	Ru(3)–H(2)	1.91 (8)
Pt(2)–C(9)	2.24 (1)	Ru(4)–C(41)	1.85 (1)
Pt(2)–C(10)	2.22 (1)	Ru(4)–C(42)	1.84 (1)
Pt(2)–C(13)	2.21 (1)	Ru(4)–C(43)	2.27 (1)
Pt(2)–C(14)	2.21 (1)	Ru(4)–H(1)	1.81 (8)
Ru(1)–Ru(2)	2.817 (1)	Ru(4)–H(2)	1.76 (8)
Ru(1)–Ru(3)	3.052 (1)	C(1)–C(2)	1.34 (1)
Ru(1)–Ru(4)	2.960 (2)	C(5)–C(6)	1.39 (1)
Ru(1)–C(17)	1.88 (1)	C(9)–C(10)	1.39 (2)
Ru(1)–C(18)	1.91 (1)	C(13)–C(14)	1.35 (2)
Ru(1)–C(19)	1.94 (1)	O–C(av)	1.14 (1)
Ru(1)–H(1)	1.83 (8)		

[a] Estimated standard deviations in the least significant figure are given in parentheses.

Table X. Intramolecular Bond Angles (deg) for **4**[a]

Ru(1)–Pt(1)–Ru(2)	59.92 (3)	Pt(2)–Ru(2)–Ru(1)	58.72 (3)
Ru(1)–Pt(1)–Ru(4)	65.36 (3)	Pt(2)–Ru(2)–Ru(4)	103.74 (4)
Ru(2)–Pt(1)–Ru(4)	65.67 (3)	Ru(1)–Ru(2)–Ru(4)	61.22 (3)
Ru(1)–Pt(2)–Ru(2)	62.52 (3)	Pt(2)–Ru(3)–Ru(4)	107.65 (4)
Ru(1)–Pt(2)–Ru(3)	66.31 (3)	Pt(1)–Ru(4)–Ru(1)	59.50 (2)
Ru(2)–Pt(2)–Ru(3)	65.05 (3)	Pt(1)–Ru(4)–Ru(2)	59.78 (3)
Pt(1)–Ru(1)–Pt(2)	117.82 (3)	Pt(1)–Ru(4)–Ru(3)	115.46 (4)
Pt(1)–Ru(1)–Ru(2)	60.55 (3)	Ru(1)–Ru(4)–Ru(2)	56.52 (3)
Pt(1)–Ru(1)–Ru(4)	55.15 (3)	Ru(1)–Ru(4)–Ru(3)	65.11 (3)
Pt(2)–Ru(1)–Ru(2)	58.76 (3)	Ru(2)–Ru(4)–Ru(3)	63.47 (3)
Pt(2)–Ru(1)–Ru(4)	104.55 (3)	Ru(1)–C(19)–O(19)	163 (1)
Ru(2)–Ru(1)–Ru(4)	62.26 (3)	Ru(2)–C(21)–O(21)	166 (1)
Pt(1)–Ru(2)–Pt(2)	116.80 (3)	Ru(3)–C(43)–O(43)	145 (1)
Pt(1)–Ru(2)–Ru(1)	59.53 (3)	Ru(4)–C(43)–O(43)	137 (1)
Pt(1)–Ru(2)–Ru(4)	54.55 (2)	Ru–C(av)–O	178 (1)

[a] Estimated standard deviations in the least significant figure are given in parentheses.

platinum atoms, and each of these platinum atoms contains one linear terminal carbonyl ligand. The tendency of platinum to form triangular $Pt_3(CO)_3$ layers in high-nuclearity cluster complexes of ruthenium and osmium has been observed previously (e.g. $Pt_4Ru_5(CO)_{20}(COD)$,[8] $Pt_4Os_6(CO)_{22}(COD)$,[18] and $Pt_4Os_6(CO)_{21}(COD)(\mu\text{-}H)_2$[7]. One platinum atom, Pt(5), containing a COD ligand was combined with two ruthenium atoms, Ru(4) and Ru(5), to form one of the outer triangles of the bioctahedon, and the remaining platinum atom with a COD ligand is a capping group on the Pt(1), Ru(4), Ru(5) triangle. Each ruthenium atom contains three linear terminal carbonyl ligands. With two hydride ligands the molecule contains a total of 136 valence electrons which is the value expected for a capped face-shared bioctahedron of ten metal atoms.[15] However, at room temperature no signal was observed in the hydride region of the ^1H NMR spectrum. Thus, a search by variable-temperature NMR spectroscopy was conducted and this revealed two resonances, δ = −18.46 and −23.82 ppm, at −80 °C that we attribute to the two inequivalent hydride ligands. These ligands undergo dynamical exchange at higher temperatures because the resonances broaden and collapse into the baseline. Interestingly, the intensity of the resonance at −23.82 ppm is only about two-thirds that of the resonance at −18.46 ppm at −80 °C. We suspect that the missing intensity of the higher field resonance exists in unobserved satellite resonances due to a short-range large coupling to ^{195}Pt (34% natural abundance), and due to the dynamical exchange process these satellites have not yet appeared at −80 °C. The lower field resonance −18.46 ppm could exhibit its full unit intensity at this temperature if it did not possess a significant coupling to platinum.

(18) (a) Adams, R. D.; Lii, J. C.; Wu, W. *Inorg. Chem.* **1991**, *30*, 2257. (b) Adams, R. D.; Lii, J. C.; Wu, W. *Inorg. Chem.* **1992**, *31*, 2556.

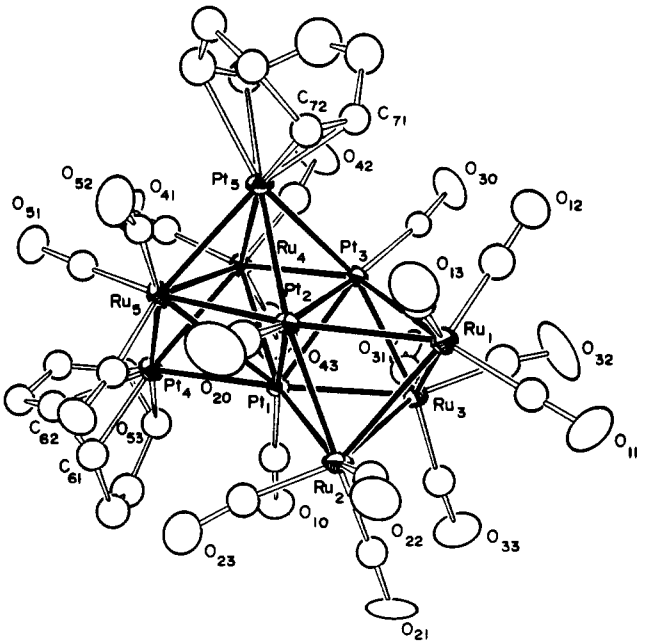

Figure 4. ORTEP diagram of $Ru_5Pt_5(CO)_{18}(COD)_2(\mu_3\text{-}H)_2$ (**5**) showing 50% probability thermal ellipsoids.

Table XI. Positional Parameters and *B*(eq) Values for **5**

atom	*x*	*y*	*z*	*B*(eq)[a] (Å²)
Pt(1)	0.72510 (9)	0.1651	0.94593 (10)	2.10 (5)
Pt(2)	0.61510 (11)	0.07448 (12)	0.75333 (12)	2.04 (5)
Pt(3)	0.61741 (11)	0.23227 (12)	0.73426 (12)	2.02 (5)
Pt(4)	0.97657 (9)	0.13565 (12)	1.04752 (10)	2.62 (5)
Pt(5)	0.72316 (9)	0.13888 (13)	0.62147 (10)	2.55 (5)
Ru(1)	0.39327 (18)	0.1628 (2)	0.6889 (2)	2.9 (1)
Ru(2)	0.5274 (2)	0.0787 (2)	0.9145 (2)	2.7 (1)
Ru(3)	0.5269 (2)	0.2673 (2)	0.8878 (3)	2.7 (1)
Ru(4)	0.8718 (2)	0.2401 (2)	0.8522 (3)	2.3 (1)
Ru(5)	0.8623 (3)	0.06182 (19)	0.8388 (3)	2.5 (1)

[a] $B_{eq} = 8\pi^2/3\sum_{i=1}^{3}\sum_{j=1}^{3}U_{ij}a_i^*a_j^*\bar{a}_i\bar{a}_j$. See: Fischer, R. X.; Tillmanns, E. *Acta Crystallogr.* **1988**, *C44*, 775.

Table XII. Intramolecular Distances (Å) for **5**[a]

Pt(1)–Pt(2)	2.678 (2)	Ru(1)–C(11)	1.88 (3)
Pt(1)–Pt(3)	2.672 (2)	Ru(1)–C(12)	1.80 (5)
Pt(1)–Pt(4)	2.827 (2)	Ru(1)–C(13)	1.91 (5)
Pt(1)–Ru(2)	2.694 (3)	Ru(2)–Ru(3)	3.114 (5)
Pt(1)–Ru(3)	2.783 (3)	Ru(2)–C(21)	1.87 (4)
Pt(1)–Ru(4)	2.854 (3)	Ru(2)–C(22)	1.86 (4)
Pt(1)–C(10)	1.82 (4)	Ru(2)–C(23)	1.87 (4)
Pt(2)–Pt(3)	2.603 (2)	Ru(3)–C(31)	1.83 (4)
Pt(2)–Pt(5)	2.779 (2)	Ru(3)–C(32)	1.86 (5)
Pt(2)–Ru(1)	2.878 (3)	Ru(3)–C(33)	1.93 (4)
Pt(2)–Ru(2)	2.720 (3)	Ru(4)–Ru(5)	2.932 (4)
Pt(2)–Ru(5)	2.757 (3)	Ru(4)–C(41)	2.00 (4)
Pt(2)–C(20)	1.86 (5)	Ru(4)–C(42)	1.93 (5)
Pt(3)–Pt(5)	2.792 (2)	Ru(4)–C(43)	1.88 (4)
Pt(3)–Ru(1)	2.805 (3)	Ru(5)–C(51)	1.85 (4)
Pt(3)–Ru(3)	2.715 (3)	Ru(5)–C(52)	1.91 (4)
Pt(3)–Ru(4)	2.822 (3)	Ru(5)–C(53)	1.91 (4)
Pt(3)–C(30)	1.93 (4)	C(61)–C(62)	1.30 (5)
Pt(4)–Ru(4)	2.829 (3)	C(65)–C(66)	1.37 (4)
Pt(4)–Ru(5)	2.695 (3)	C(71)–C(72)	1.35 (5)
Pt(5)–Ru(4)	3.172 (3)	C(71)–C(78)	1.33 (5)
Pt(5)–Ru(5)	2.840 (3)	C(75)–C(76)	1.39 (5)
Ru(1)–Ru(2)	2.960 (4)	O–C(av)	1.15 (5)
Ru(1)–Ru(3)	2.903 (4)		

[a] Estimated standard deviations in the least significant figure are given in parentheses.

Table XIII. Intramolecular Bond Angles (deg) for **5**[a]

Pt(2)–Pt(1)–Pt(4)	109.63 (6)	Pt(5)–Pt(3)–Ru(1)	108.22 (8)
Pt(2)–Pt(1)–Ru(3)	93.43 (8)	Pt(5)–Pt(3)–Ru(3)	157.7 (1)
Pt(2)–Pt(1)–Ru(4)	90.64 (7)	Ru(1)–Pt(3)–Ru(4)	153.1 (1)
Pt(3)–Pt(1)–Pt(4)	119.38 (6)	Ru(3)–Pt(3)–Ru(4)	108.6 (1)
Pt(3)–Pt(1)–Ru(2)	93.06 (8)	Pt(3)–Pt(5)–Ru(5)	87.55 (8)
Pt(4)–Pt(1)–Ru(2)	135.77 (9)	Pt(2)–Ru(1)–Ru(3)	86.91 (8)
Pt(4)–Pt(1)–Ru(3)	151.99 (9)	Pt(3)–Ru(1)–Ru(2)	84.95 (8)
Ru(2)–Pt(1)–Ru(4)	149.9 (1)	Pt(1)–Ru(2)–Ru(1)	88.8 (1)
Ru(2)–Pt(1)–C(10)	94 (1)	Pt(2)–Ru(2)–Ru(3)	85.6 (1)
Ru(3)–Pt(1)–Ru(4)	105.8 (1)	Pt(1)–Ru(3)–Ru(1)	88.3 (1)
Pt(1)–Pt(2)–Pt(5)	99.38 (6)	Pt(3)–Ru(3)–Ru(2)	83.5 (1)
Pt(1)–Pt(2)–Ru(1)	90.89 (8)	Pt(3)–Ru(4)–Pt(4)	114.3 (1)
Pt(3)–Pt(2)–Ru(2)	94.03 (9)	Pt(3)–Ru(4)–Ru(5)	85.2 (1)
Pt(3)–Pt(2)–Ru(5)	93.22 (8)	Pt(2)–Ru(5)–Pt(4)	111.3 (1)
Pt(5)–Pt(2)–Ru(1)	106.54 (8)	Pt(2)–Ru(5)–Ru(4)	87.5 (1)
Pt(5)–Pt(2)–Ru(2)	155.3 (1)	Pt(4)–Ru(5)–Pt(5)	126.6 (1)
Ru(1)–Pt(2)–Ru(5)	153.8 (1)	Ru(1)–C(13)–O(13)	166 (4)
Ru(2)–Pt(2)–Ru(5)	116.2 (1)	Ru(2)–C(22)–O(22)	164 (4)
Pt(1)–Pt(3)–Pt(5)	99.22 (6)	Ru(2)–C(23)–O(23)	166 (3)
Pt(1)–Pt(3)–Ru(1)	92.63 (7)	Ru(5)–C(52)–O(52)	164 (4)
Pt(2)–Pt(3)–Ru(3)	96.76 (9)	M–C(av)–O	174 (4)
Pt(2)–Pt(3)–Ru(4)	92.92 (8)		

[a] Estimated standard deviations in the least significant figure are given in parentheses.

The hydride ligands were not located directly in this structural analysis; however, the bonds joining two pairs of metal atoms on the outer triangles of the bioctahedron are much longer than all of the other metal–metal bonds, Ru(2)–Ru(3) = 3.114 (5) Å and Pt(5)–Ru(4) = 3.172 (3) Å. It is well-known that hydride ligands produce a diagnostic lengthening of the metal–metal bonds that they bridge.[14] Accordingly, we believe that the hydride ligands are strongly associated with these elongated metal–metal bonds, but they might also lean over the outer triangular faces to assume a semitriply bridging character.

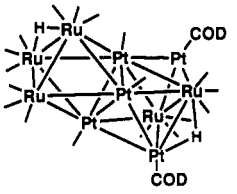

5

Scheme I

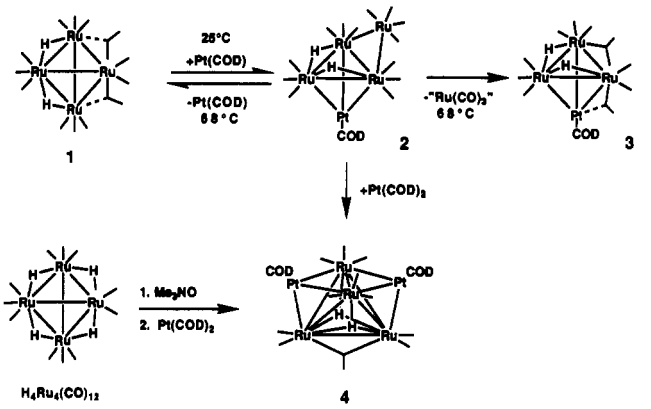

Discussion

The results of this study are summarized in Scheme I. $Pt(COD)_2$ reacts with $Ru_4(CO)_{13}(\mu\text{-}H)_2$ (**1**) by loss of a COD ligand and addition of Pt(COD) to **1** to yield the opened Ru_4 cluster grouping in compound **2**. The Pt(COD) group becomes a capping group on one of the Ru_3 triangles. When heated, **2** is transformed in low yields to the two new mixed-metal complexes **3** and **4** while a significant amount of **1** is regenerated by elimination of the Pt(COD) and a closing of the Ru_4 butterfly. When heated in the presence of $Pt(COD)_2$, the yield of **3** increased. There were fewer trace side products and no **1** was regenerated; unfortunately, the amount of **4** did not increase significantly.

A small amount of the interesting high-nuclearity complex **5** was also obtained from the reaction of $Pt(COD)_2$ with **1**. We have not yet been able to devise a good yield synthesis for **5**, and thus we have not been able to investigate it further. All of the reactions involving $Pt(COD)_2$ produce large amounts of uncharacterizable black residues.

Acknowledgment. These studies were supported by the National Science Foundation under Grant No. CHE-8919786.

Supplementary Material Available: Tables of positional, parameters, bond angles, and anisotropic thermal parameters for all four structural analyses (30 pages). Ordering information is given on any current masthead page.